Ambipolar all-polymer bulk heterojunction field-effect transistors

Szendrei, Krisztina; Jarzab, Dorota; Chen, Zhihua; Facchetti, Antonio; Loi, Maria A.

Published in:
Journal of Materials Chemistry

DOI:
10.1039/b919596c

Publication date:
2010

Ambipolar all-polymer bulk heterojunction field-effect transistors†

Krisztina Szendrei,[a] Dorota Jarzab,[a] Zhihua Chen,[b] Antonio Facchetti*[b] and Maria A. Loi*[a]

Received 21st September 2009, Accepted 6th November 2009
First published as an Advance Article on the web 3rd December 2009
DOI: 10.1039/b919596c

We demonstrate solution processable all-polymer based field-effect transistors (FETs) exhibiting comparable electron and hole mobilities. The semiconducting layer is a bulk heterojunction of poly{[*N*,*N*′-bis(2-octyldodecyl)-naphthalene-1,4,5,8-bis(dicarboximide)-2,6-diyl]-alt-5,5′-(2,2′-bithiophene)} (n-type polymer) and regioregular poly(3-hexylthiophene) (p-type polymer). These polymers form a type-II heterojunction as revealed by the faster photoluminescence dynamics of the blend compared to the pristine materials. An electron mobiliy of 4×10^{-3} cm^2/V s and a hole mobility of 2×10^{-3} cm^2/V s were extracted from the transfer characteristics of bottom contact FETs. The balanced mobilities suggest that the active layer is a fine network of the two components, as confirmed by atomic force microscopy phase images.

Introduction

Organic semiconductor films which can efficiently transport both holes and electrons, have great potential for the realization of ambipolar field-effect transistors (FETs),[1–28] organic complementary technologies (O-CMOS),[5,9] and organic light emitting transistors (OLETs).[1–3] These devices provide a unique opportunity to enable low-cost, solution processable, roll-to-roll manufactured electronics. In the last few years, ambipolar organic FETs have been fabricated using single components,[4–12] bilayers,[13–20] and blends[1–3,5,21–28] as semiconducting active layers. One of the major challenges in achieving good FET ambipolar transport is the efficient injection of holes and electrons from the same metal electrode, since this electrode must inject both electrons into the LUMO (lowest unoccupied molecular orbital) and holes into the HOMO (highest occupied molecular orbital) of the semiconductor(s). The band gaps of most organic semiconductors are typically ~2–3 eV, resulting in a high injection barrier for at least one type of charge carrier, when a single electrode material is employed. The combination of two organic semiconductors in a bilayer or bulk heterojunction provides a great opportunity to overcome this limitation. In either case, if the materials are warily chosen, the work function of the electrodes could line up properly with the HOMO of one semiconductor for hole injection and with the LUMO of the other for electron injection. The idea of using bilayers composed of an n-type and a p-type semiconducting material to achieve ambipolar FETs was first introduced by Dodabalapur *et al.*, who demonstrated FET mobilities up to 0.005 cm^2/V s for electrons and 0.004 cm^2/V s for holes.[13] Several studies[14–20] have recently shown that the combination of n/p-type semiconducting bilayers in organic FETs can lead to excellent ambipolar performance, with mobility values up to 0.23 cm^2/V s for electrons and 0.14 cm^2/V s for holes.[18] In all of these reports the active layer was deposited by thermal evaporation. In fact, solution processed bilayer films are difficult to realize since they require that the second layer is processable from an orthogonal solvent to the one of the first layer. Thus, p/n-channel semiconducting bulk heterojunctions can be an alternative way to realise ambipolar transport in a single layer. This strategy has been successfully demonstrated for both solution processed and vacuum sublimed semiconducting layers.[1,2,21–28] Ambipolar organic FETs based on a solution processable mixture of two organic semiconductors were first demonstrated by Tada *et al.* in 1996, unfortunately, resulting in low charge carrier mobilities (10^{-7} cm^2/V s for holes and 10^{-9} cm^2/V s for electrons).[21] More recently, even if the reported carrier mobilities never exceeded the 10^{-3} cm^2/V s range, it was shown that using blends is a promising way to realise ambipolar transport in a single layer.[2,5,22–25,28] However, there are only a few examples in the literature where all-polymer bulk heterojunctions are used to fabricate FETs. In a recent report a hole mobility of ~10^{-4} cm^2/V s and an electron mobility of ~10^{-5} cm^2/V s were obtained by using a blend of poly(benzobisimidazobenzophenanthroline) (n-type polymer) and ~98% by weight of poly[(thiophene-2,5-diyl)-*alt*-(2,3-diheptylquinoxaline-5,8-diyl)] (p-type polymer).[28] The limited number of polymer–polymer heterojunctions is due to the scarcity of high-performing and soluble n-type polymers. Consequently, most often either fullerenes[5,23–25,27] or other small molecules[1,2,26] are used as n-type semiconductors in bulk heterojunctions. The recent discovery of the n-type polymer poly{[*N*,*N*′-bis(2-octyldodecyl)-naphthalene-1,4,5,8-bis(dicarboximide)-2,6-diyl]-alt-5,5′-(2,2′-bithiophene)} (P(NDI2OD-T2)),[29] exhibiting large electron mobilities in ambient conditions, may enable the development of efficient polymer-based bulk heterojunction ambipolar FETs.

Here we demonstrate the fabrication of solution processed all-polymer bulk heterojunction ambipolar transistors with high and balanced hole and electron mobilities. The active layer is based on the bulk heterojunction of P(NDI2OD-T2) and rr-P3HT as n- and p-type semiconductors, respectively. The devices are fabricated in a bottom gate/bottom contact configuration and exhibit

[a]*Physics of Organic Semiconductors, Zernike Institute for Advanced Materials, University of Groningen, Nijenborgh 4, 9700 AE Groningen, The Netherlands. E-mail: M.A.Loi@rug.nl; Fax: +31(0)50-3638751*
[b]*Polyera Corporation, Skokie, 8025 Lamon Avenue, IL 60077, USA*
† This paper is part of a *Journal of Materials Chemistry* issue highlighting the work of emerging investigators in materials chemistry.

comparable n-type and p-type mobilities (2–4 $\times$ 10^{-3} cm^2/V s). These are the best performing devices, ever reported in the class of all-polymer bulk heterojunction FETs and are one of the few examples[2,23,25,27] of balanced ambipolar charge transport in organic semiconductors. The morphological characterisation of the bulk heterojunction thin film and its components provides deeper insights on the origin of the high performance of these ambipolar devices. Moreover, the photophysical studies evidence that the two polymers form a type-II heterojunction, indicating the possibility to achieve photoinduced charge generation, thus opening new opportunities for the fabrication of other opto-electronic devices.

Experimental section

P(NDI2OD-T2)

The (NDI) naphthalene-bis(dicarboximide)-based poly{[*N*,*N*′-bis(2-octyldodecyl)-naphthalene-1,4,5,8-bis(dicarboximide)-2,6-diyl]-alt-5,5′-(2,2′-bithiophene)}, (P(NDI2OD-T2)), (see Fig. 1) is commercially available from Polyera Corporation under the trade name of ActivInk N2200. For this study, a batch having a M_w of ~250 Kda and a PDI of ~5 was used. P(NDI2OD-T2) is highly soluble in chlorinated solvents, toluene and xylene (~60 mg ml^{-1} at room temperature) and exhibits electron mobilities >0.45 cm^2/V s in a top-gate FET configuration.[29] The LUMO and HOMO energy levels of P(NDI2OD-T2) are ~4.0 eV and ~5.6 eV below the vacuum level, respectively.[29]

rr-P3HT

Regioregular poly(3-hexylthiophene) (rr-P3HT), (see Fig. 1), with regioregularity of 98.5%, was purchased from Rieke Metals. This polymer is one of the most widely investigated p-type semiconductors with reported hole mobilities up to 0.1 cm^2/V s.[30–32] The HOMO and LUMO energy levels of rr-P3HT are located ~4.8 eV and ~3.0 eV below the vacuum level.

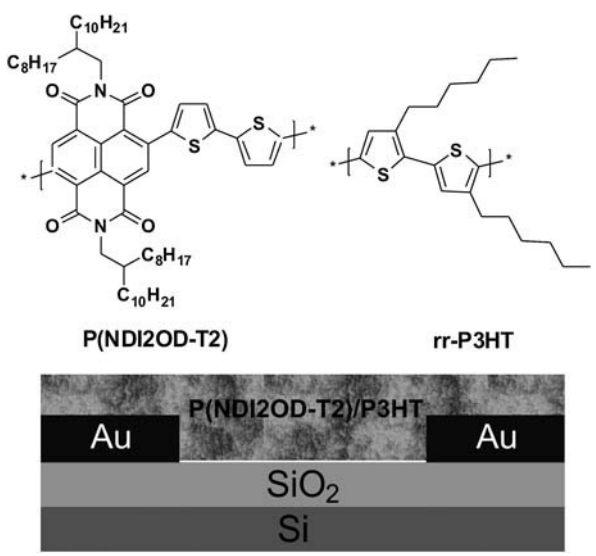

Fig. 1 Chemical structure of the semiconducting polymers P(NDI2OD-T2) and rr-P3HT and illustration of the bottom-gate/bottom-contact (BG/BC) FET architecture employed in this study.

Device fabrication and electrical measurements

Bottom gate/bottom contact FETs (see Fig. 1) were fabricated using a heavily doped silicon wafer as the gate electrode with a 200 nm thick layer of thermally grown SiO_2 functioning as the gate dielectric (capacitance = 17 $nFcm^{-2}$). The source and drain electrodes consist of 10 nm of Ti coated with 100 nm of Au. An interdigitated electrode configuration with typical length L = 5–20 μm and width W = 10 000 μm (W L^{-1} = 500–2000) was used. The silicon oxide surface was treated with HMDS (hexamethyldisilazane) to form a hydrophobic monolayer coating following a procedure reported previously.[33] The Au electrodes were either untreated or treated with 1-hexadecanethiol and 3,5-bis(trifluoromethyl)-benzenethiol to tune the gold surface energy and improve surface wettability. The semiconductor blend of P(NDI2OD-T2) and rr-P3HT (typically in the proportion of 1 : 1 by weight) was spin cast onto the interdigitated electrodes from a 1,2-orthodichlorobenzene (ODCB) solution. The solution was magnetically stirred overnight and filtered through a 0.5 μm polytetrafluoroethylene (PTFE) syringe filter prior to deposition. To avoid contamination from oxygen and water, the polymer blend was spin cast in a nitrogen filled glove box. Subsequently, the devices were placed in a vacuum oven and annealed overnight at 110 °C. Electrical measurements, approximately on 50 devices, were carried out in a probe station under vacuum conditions (10^{-6} mbar) and ambient temperature with a Keithley 4200 semiconductor analyser. Note that devices fabricated with and without Au thiol functionalization were studied, but they showed no significant difference. Therefore, in the following sections, the untreated devices are discussed.

Optical and surface characterisations

Absorption measurements were performed with a Perkin Elmer Lambda 900 spectrometer. The steady-state and time-resolved photoluminescence (PL) measurements were performed by photoexciting the thin films with a 150 fs pulse Kerr mode locked Ti–sapphire laser doubled at 380 nm. The steady-state PL was measured in the near infrared with an InGaAs detector from Andor and in the visible with a Si-CCD from Hamamatsu. The time-resolved PL of the thin films of the two polymers and the bulk heterojunction was recorded by two Hamamatsu streak cameras working in synchroscan mode, one with a photocathode sensitive in the visible and the other in the near infrared spectral range. All of the measurements were performed at room temperature. Atomic force microscopy (AFM) images of the P(NDI2OD-T2)/rr-P3HT active layer were recorded with a MultiMode AFM NanoScope IV Scanning Probe Microscope Controller functioning in tapping mode.

Results and discussion

Ambipolar FETs based on a bulk heterojunction of two materials require the mixing of high mobility p- and n-type semiconductors. The chemical structures of the n-type (P(NDI2OD-T2)) and the p-type (rr-P3HT) polymers chosen for the purpose of this study are shown in Fig. 1. In addition, efficient injection of both charge carriers from the metal electrode into the LUMO level of P(NDI2OD-T2) and HOMO level of rr-P3HT is necessary. Fig. 2 shows the schematic energy level diagram of the semiconducting

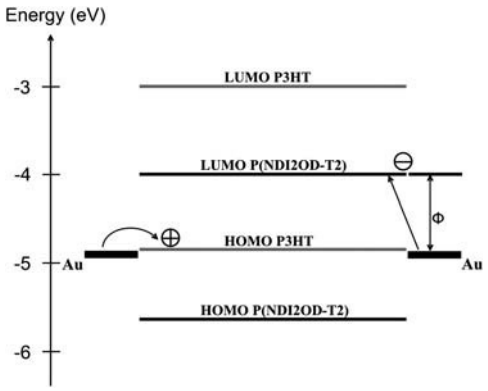

Fig. 2 Schematic energy level diagrams of P(NDI2OD-T2) and rr-P3HT with respect to the work function of Au contacts.

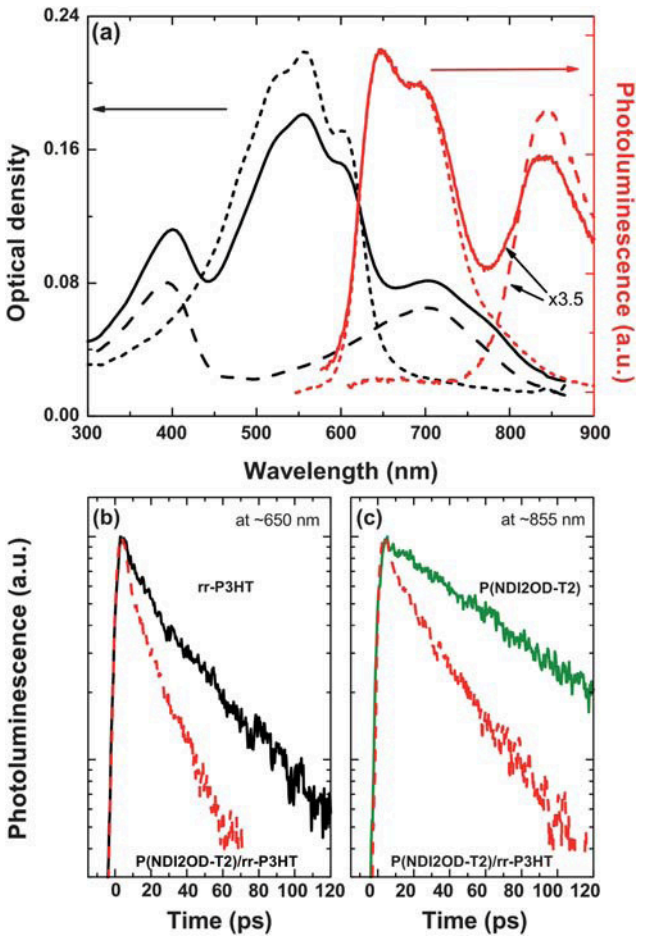

Fig. 3 (a) Optical density and the photoluminescence spectra of rr-P3HT (dashed lines) and P(NDI2OD-T2) (large dashed lines) and P(NDI2OD-T2)/rr-P3HT (continuous lines) thin films. (b) Time-resolved PL of rr-P3HT and P(NDI2OD-T2)/rr-P3HT thin films measured at 650 nm. (c) Time-resolved PL of P(NDI2OD-T2) and P(NDI2OD-T2)/rr-P3HT thin films measured at 855 nm.

polymers used in this study with respect to the Au source and drain electrodes. The energy levels are represented as straight lines, not taking into account the band bending which occurs at the insulator–polymer interface when the gate bias is applied. Clearly, the HOMO level of rr-P3HT (4.8 eV) is close to the work function of the gold electrodes (~4.9 eV).[34] This allows the efficient injection of holes into the HOMO level of rr-P3HT without any significant barrier. On the other hand, the relative position of the LUMO level of P(NDI2OD-T2) with respect to the gold work function cannot be considered as an Ohmic contact due to the presence of an injection barrier (ϕ) of ~0.9 eV. However, in our experiments the electron injection is only slightly limited (*vide infra*). Recently, it has been shown that similar barriers can be reduced through the formation of an interface dipole at the metal/semiconductor interface.[35] In addition, the injection barrier can be further reduced by the application of the perpendicular gate and the lateral source–drain electric fields.[36]

Fig. 3(a) displays the optical density (OD) and the photoluminescence spectra of rr-P3HT, P(NDI2OD-T2) and P(NDI2OD-T2)/rr-P3HT bulk heterojunction thin films. The OD spectrum of the blend is a superposition of the ones of the component materials. The blend absorbs in the whole visible range, from 350 nm to 750 nm. Three main absorption bands can be distinguished, two originating from P(NDI2OD-T2) that are centred at ~395 nm and ~700 nm and one originating from rr-P3HT, centred at ~550 nm. Also, the PL spectrum of the blend consists of two bands stemming from those of the two components. The PL spectrum of the pristine rr-P3HT film shows two vibronic peaks centred at ~650 nm and ~700 nm with a shoulder at ~800 nm. The PL spectrum of P(NDI2OD-T2) is characterized by a single peak at 850 nm. By mixing the two polymers there is no apparent influence on the spectral shape and energy of the blend emission features. The only evident difference in the optical properties of the bulk heterojunction with respect to the two separate polymer thin films is the overall reduction of the PL intensity. The rr-P3HT and P(NDI2OD-T2) emission intensities in the blend are reduced by ~3.5× and ~1.5×, respectively. Time-resolved PL measurements are reported in Fig. 3(b) and (c). Fig. 3(b) shows the PL dynamics of rr-P3HT and of the P(NDI2OD-T2)/rr-P3HT blend detected at ~650 nm, which corresponds to the rr-P3HT 0–0 transition. At this wavelength both samples show a bi-exponential decay with the second time constant significantly larger than the first one. The PL lifetime of the rr-P3HT can be fit with time constants $\tau_1 \approx 41$ ps and $\tau_2 \approx 142$ ps, while for the blend the time constants are $\tau_1 \approx 21$ ps and $\tau_2 \approx 75$ ps. Fig. 3(c) shows the PL decay time for the P(NDI2OD-T2)/rr-P3HT blend and the pristine P(NDI2OD-T2) detected at ~855 nm. In this case both samples show a mono-exponential decay characterized by time constants $\tau \approx 98$ ps for the pristine polymer and $\tau \approx 54$ ps for the heterojunction. This lifetime variation is ascribed to the photoinduced electron or hole transfer in the type-II heterojunction formed by the two polymers. Thus, P(NDI2OD-T2)/rr-P3HT heterojunctions could be used as active layer for photoactive devices such as solar cells and photodetectors. Experiments in this direction are in progress. Fig. 4 and 5 show representative output and transfer plots, respectively, of the all-polymer bulk heterojunction FETs. The ambipolar nature of these FETs in both electron enhancement (Fig. 4(a)) and hole enhancement (Fig. 4(b)) modes is evident. At high positive gate voltages (V_G) these transistors function in the n-channel operation mode with increasing positive V_{DS}, similarly to the unipolar P(NDI2OD-T2) FETs when only electrons are

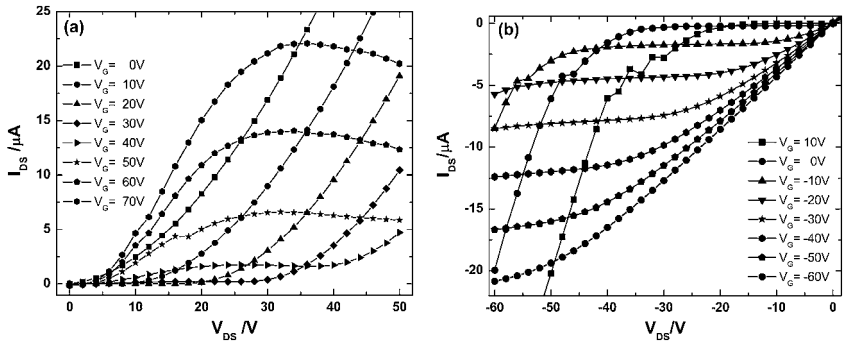

Fig. 4 Typical output characteristics of the ambipolar polymer blend FETs in (a) n-type operation mode and (b) p-type operation mode.

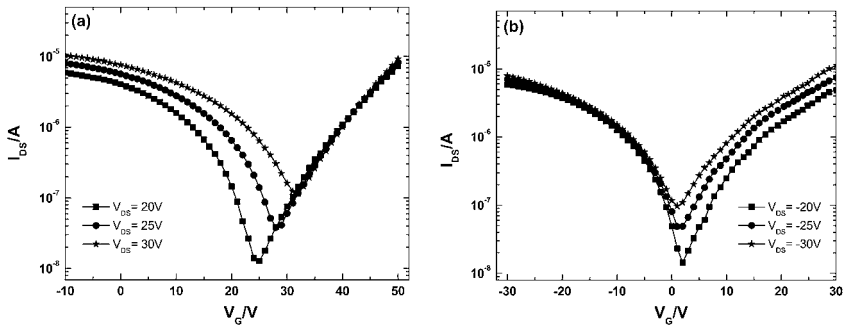

Fig. 5 Typical transfer characteristics of the ambipolar polymer blend FETs in (a) n-type operation mode and (b) p-type operation mode.

accumulated at the semiconductor–insulator interface. It is noticeable that at low V_{DS} the output curves show clear indications of contact resistance for electron injection. For lower V_G the devices are ambipolar, showing the typical non-linear increase in current at high V_{DS} due to the injection of both charge carriers in the channel (Fig. 4(a)). A similar behavior is observed when applying negative V_G and V_{DS} biases (Fig. 4(b)). However, the current is far less limited for hole injection, in agreement with the ohmic nature of the contact between Au and the HOMO level of rr-P3HT (Fig. 2).

Fig. 5(a) and (b) show the transfer characteristics of these polymer FETs for positive and negative V_{DS}, respectively. In both cases the transfer shows a symmetric shape, indicative of well balanced electron and hole populations in the channel. The current on-off ratios of these FETs are very large and surpass $\sim 10^3$, which is among the best values reported so far for ambipolar transistors. The threshold voltages are $\sim$+25 V for n-type operation (Fig. 5(a)) and $\sim$+2 V for p-type operation (Fig. 5(b)). The high threshold voltage for n-channel operation is probably due to a combination of charge injection limited contact and electron trapping at the semiconductor–dielectric interface. Note that the use of hydroxyl-free gate dielectric substantially reduces the threshold voltages in top-gate P(NDI2OD-T2) TFTs.[29] Thus, a similar approach, could be used for these blends to improve performance.

The charge carrier mobilities (μ) of these devices were extracted from the drain–source current (I_{DS}) *versus* gate voltage (V_G) data in the saturation regime using the formula:

$$\mu = \frac{2L}{WC_i}\left(\frac{\partial\sqrt{I_{DS}}}{\partial V_{GS}}\right)^2 \quad (1)$$

where L is the channel length, W is the channel width and C_i is the gate dielectric capacitance per unit area. According to eqn (1) our ambipolar transistors exhibit an n-type saturation mobility of 4×10^{-3}cm^2/V s at $V_{DS} = +30$ V and a p-type mobility of 2×10^{-3} cm^2/V s at $V_{DS} = -30$ V. These mobilities are the highest balanced mobilities reported so far for solution processed all-polymer bulk heterojunction ambipolar FETs. It is also important to underline that the electron and hole mobilities in these ambipolar devices are not significantly lower than those of the unipolar FETs we have fabricated with the single polymers in the same device configuration. The mobility value measured for the reference devices are 6×10^{-3} cm^2/V s for electrons in P(NDI2OD-T2) and 4×10^{-3} cm^2/V s for holes in rr-P3HT.

The balanced FET mobilities may indicate the presence of good percolation pathways for both charge carriers in these polymer bulk heterojunctions. Therefore, the surface morphology of the blend was investigated by AFM. Fig. 6 shows

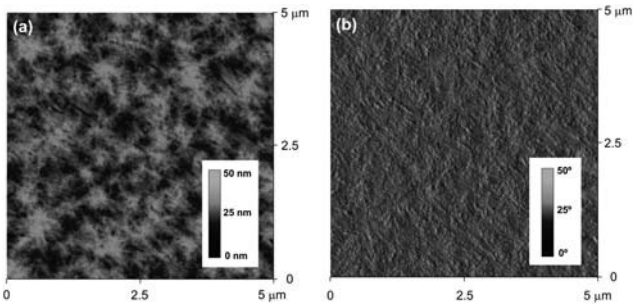

Fig. 6 Topography (a) and phase (b) images of the P(NDI2OD-T2)/rr-P3HT thin film measured on the FET active layer.

the AFM topography (a) and phase (b) of the P(NDI2OD- T2)/rr-P3HT active layer. The P(NDI2OD-T2)/rr-P3HT thin film surface is quite smooth, characterised by small protrusions and an RMS roughness of 3.9 nm. The phase image (Fig. 6(b)) shows a very fine network of materials with two different phases, suggesting phase segregation between P(NDI2OD-T2) and rr-P3HT. This fine network, characterized by a dendrimeric shape, is in agreement with the presence of efficient percolation pathways for both charge carriers, supporting the good ambipolarity of the bulk heterojunction.

Conclusion

We have demonstrated high performance organic ambipolar FETs based on a P(NDI2OD-T2)/rr-P3HT polymer bulk heterojunction as the semiconductor layer. The two polymers form a type-II heterojunction, resulting in the photogeneration of charges as shown by time resolved photoluminescence measurements. The devices fabricated in bottom contact/bottom gate configuration exhibit balanced electron and hole charge carrier mobilities. The extracted values are 4×10^{-3} cm^2/V s for electrons and 2×10^{-3} cm^2/V s for holes with I_{on}/I_{off} ratios of $\geq 10^3$, which are the highest reported so far for polymer bulk heterojunction-based FETs. The large ambipolarity and optical characteristics of this bulk heterojunction may hold promise for future opto-electronic applications.

Acknowledgements

K. Sz. and M. A. L. acknowledge P. W. M. Blom for support and C. Piliego for discussions. J. Harkema and F. van der Horst are acknowledged for their technical assistance. The work in Groningen was funded by the European Commission through the Human Potential Programs (RTN Nanomatch, Contract No. MRTN-CT-2006-035884).

References

1 C. Rost, S. Karg, W. Riess, M. A. Loi, M. Murgia and M. Muccini, *Appl. Phys. Lett.*, 2004, **85**, 1613.
2 M. A. Loi, C. Rost-Bietsch, M. Murgia, S. Karg, W. Riess and M. Muccini, *Adv. Funct. Mater.*, 2006, **16**, 41–47.
3 J. Zaumseil and H. Sirringhaus, *Chem. Rev.*, 2007, **107**, 1296–1323.
4 L. Chua, J. Zaumseil, J. Chang, E. C. Ou, P. K. Ho, H. Sirringhaus and R. H. Friend, *Nature*, 2005, **434**, 194–199.
5 E. J. Meijer, D. M. de Leeuw, S. Setayesh, E. van Veenendaal, B.-H. Huisman, P. W. M. Blom, J. C. Hummelen, U. Scherf and T. M. Klapwijk, *Nat. Mater.*, 2003, **2**, 678–682.
6 T. D. Anthopoulos, C. Tanase, S. Setayesh, E. J. Meijer, J. C. Hummelen, P. W. M. Blom and D. M. de Leeuw, *Adv. Mater.*, 2004, **16**, 2174–2179.
7 R. W. I. de Boer, A. F. Stassen, M. F. Craciun, C. L. Mulder, A. Molinari, S. Rogge and A. F. Morpurgo, *Appl. Phys. Lett.*, 2005, **86**, 262109–3.
8 T. B. Singh, F. Meghdadi, S. Günes, N. Marjanovic, G. Horowitz, P. Lang, S. Bauer and N. S. Sariciftci, *Adv. Mater.*, 2005, **17**, 2315–2320.
9 T. D. Anthopoulos, S. Setayesh, E. Smits, M. Cölle, E. Cantatore, B. de Boer, P. W. M. Blom and D. M. de Leeuw, *Adv. Mater.*, 2006, **18**, 1900–1904.
10 R. Schmechel, M. Ahles and H. von Seggern, *J. Appl. Phys.*, 2005, **98**, 084511–6.
11 E. C. P. Smits, T. D. Anthopoulos, S. Setayesh, E. van Veenendaal, R. Coehoorn, P. W. M. Blom, B. de Boer and D. M. de Leeuw, *Phys. Rev. B: Condens. Matter Mater. Phys.*, 2006, **73**, 205316–9.
12 S. Z. Bisri, T. Takenobu, Y. Yomogida, H. Shimotani, T. Yamao, S. Hotta and Y. Iwasa, *Adv. Funct. Mater.*, 2009, **19**, 1728–1735.
13 A. Dodabalapur, H. E. Katz, L. Torsi and R. C. Haddon, *Science*, 1995, **269**, 1560–1562.
14 C. Rost, D. J. Gundlach, S. Karg and W. Riess, *J. Appl. Phys.*, 2004, **95**, 5782–5787.
15 J. Wang, H. Wang, X. Yan, H. Huang and D. Yan, *Appl. Phys. Lett.*, 2005, **87**, 093507–3.
16 R. Ye, M. Baba, Y. Oishi, K. Mori and K. Suzuki, *Appl. Phys. Lett.*, 2005, **86**, 253505–3.
17 F. Dinelli, R. Capelli, M. A. Loi, M. Murgia, M. Muccini, A. Facchetti and T. J. Marks, *Adv. Mater.*, 2006, **18**, 1416–1420.
18 S. Wang, K. Kanai, Y. Ouchi and K. Seki, *Org. Electron.*, 2006, **7**, 457–464.
19 H. Wang, J. Wang, X. Yan, J. Shi, H. Tian, Y. Geng and D. Yan, *Appl. Phys. Lett.*, 2006, **88**, 133508–3.
20 Z. Wei, W. Xu, W. Hu and D. Zhu, *J. Mater. Chem.*, 2008, **18**, 2420–2422.
21 K. Tada, H. Harada and K. Yoshino, *Jpn. J. Appl. Phys.*, 1996, **35**, L944–L946.
22 A. Babel, J. D. Wind and S. A. Jenekhe, *Adv. Funct. Mater.*, 2004, **14**, 891–898.
23 M. Shkunov, R. Simms, M. Heeney, S. Tierney and I. McCulloch, *Adv. Mater.*, 2005, **17**, 2608–2612.
24 Y. Hayashi, H. Kanamori, I. Yamada, A. Takasu, S. Takagi and K. Kaneko, *Appl. Phys. Lett.*, 2005, **86**, 052104.
25 S. Cho, J. Yuen, J. Y. Kim, K. Lee and A. J. Heeger, *Appl. Phys. Lett.*, 2006, **89**, 153505.
26 K. N. Unni, A. K. Pandey, S. Alem and J. Nunzi, *Chem. Phys. Lett.*, 2006, **421**, 554–557.
27 M. Bronner, A. Opitz and W. Brütting, *Phys. Status Solidi A*, 2008, **205**, 549–563.
28 A. Babel, Y. Zhu, K. Cheng, W. Chen and S. Jenekhe, *Adv. Funct. Mater.*, 2007, **17**, 2542–2549.
29 H. Yan, Z. Chen, Y. Zheng, C. Newman, J. R. Quinn, F. Dotz, M. Kastler and A. Facchetti, *Nature*, 2009, **457**, 679–686.
30 Z. Bao, A. Dodabalapur and A. J. Lovinger, *Appl. Phys. Lett.*, 1996, **69**, 4108.
31 H. Sirringhaus, N. Tessler and R. H. Friend, *Science*, 1998, **280**, 1741–1744.
32 H. Sirringhaus, P. J. Brown, R. H. Friend, M. M. Nielsen, K. Bechgaard, B. M. W. Langeveld-Voss, A. J. H. Spiering, R. A. J. Janssen, E. W. Meijer, P. Herwig and D. M. de Leeuw, *Nature*, 1999, **401**, 685–688.
33 C. Piliego, D. Jarzab, G. Gigli, Z. Chen, A. Facchetti and M. A. Loi, *Adv. Mater.*, 2009, **21**, 1573–1576.
34 B. de Boer, A. Hadipour, M. M. Mandoc, T. van Woudenbergh and P. W. M. Blom, *Adv. Mater.*, 2005, **17**, 621–625.
35 H. Ishii, K. Sugiyama, E. Ito and K. Seki, *Adv. Mater.*, 1999, **11**, 605–625.
36 S. M. Sze, *Physics of Semiconductor Devices*, Wiley, New York, 1981.